

Arteriosclerosis, Thrombosis, and Vascular Biology

JOURNAL OF THE AMERICAN HEART ASSOCIATION



The ACAT Inhibitor Avasimibe Reduces Macrophages and Matrix Metalloproteinase Expression in Atherosclerotic Lesions of Hypercholesterolemic Rabbits

Thomas M. A. Bocan, Brian R. Krause, Wendy S. Rosebury, Sandra Bak Mueller, Xiaokang Lu, Catherine Dagle, Terry Major, Chetan Lathia and Helen Lee
Arterioscler. Thromb. Vasc. Biol. 2000;20:70-79

Arteriosclerosis, Thrombosis, and Vascular Biology is published by the American Heart Association,
7272 Greenville Avenue, Dallas, TX 75214

Copyright © 2000 American Heart Association. All rights reserved. Print ISSN: 1079-5642. Online ISSN: 1524-4636

The online version of this article, along with updated information and services, is located on the World Wide Web at:

<http://atvb.ahajournals.org/cgi/content/full/20/1/70>

Subscriptions: Information about subscribing to Arteriosclerosis, Thrombosis, and Vascular Biology is online at

<http://atvb.ahajournals.org/subscriptions/>

Permissions: Permissions & Rights Desk, Lippincott Williams & Wilkins, a division of Wolters Kluwer Health, 351 West Camden Street, Baltimore, MD 21202-2436. Phone: 410-528-4050. Fax: 410-528-8550. E-mail:

journalpermissions@lww.com

Reprints: Information about reprints can be found online at

<http://www.lww.com/reprints>

The ACAT Inhibitor Avasimibe Reduces Macrophages and Matrix Metalloproteinase Expression in Atherosclerotic Lesions of Hypercholesterolemic Rabbits

Thomas M.A. Bocan, Brian R. Krause, Wendy S. Rosebury, Sandra Bak Mueller, Xiaokang Lu, Catherine Dagle, Terry Major, Chetan Lathia, Helen Lee

Abstract—Given the significance of cholesteryl ester (CE) accumulation in macrophage foam cell formation, we hypothesized that inhibitors of acyl-CoA:cholesterol *O*-acyltransferase (ACAT) would produce a histologically stable lesion by limiting macrophage enrichment and thereby a source of matrix metalloproteinases (MMPs). Male New Zealand White rabbits were sequentially fed a cholesterol/fat diet for 9 weeks, a fat-only diet for 6 weeks, and 25 mg/kg avasimibe for 7 to 8 weeks. Avasimibe had no effect on plasma total cholesterol exposure. Plasma avasimibe maximal concentration and 24-hour area-under-the-curve levels were 178 ng/mL and 2525 ng · h/mL, respectively, after 7 weeks of treatment with 25 mg/kg avasimibe. The median inhibitory concentration against human monocyte-macrophage ACAT was 12 ng/mL when determined in the absence of albumin, and aortic arch avasimibe levels were 25 ng/g of tissue wet weight. Avasimibe reduced thoracic aortic and iliac-femoral CE content by 39%, the extent of thoracic aortic lesions by 41%, aortic arch cross-sectional lesions area by 35%, and monocyte-macrophage area by 27%. The reduction in monocyte-macrophage area reflected a change in cell number and not cell size. In the iliac-femoral artery, avasimibe decreased monocyte-macrophage content by 77% and reduced the macrophage-to-lesion ratio from 0.16 to 0.05. Within the aortic arch, the catalytic activity of latent and active MMP-9 was reduced by 65% and 33%, respectively; latent and active MMP-1 and MMP-3 activity measured collectively was decreased by 52% and 60%, respectively, and MMP-2 was unchanged. Aortic arch MMP-9, tissue inhibitor of matrix metalloproteinase (TIMP)-1, and TIMP-2 mRNA levels were reduced 29% to 39%, and MMP-2 mRNA levels increased. We conclude that the bioavailable ACAT inhibitor avasimibe can directly limit macrophage accumulation, resulting in the histological appearance of mainly fibromuscular lesions, and can potentially stabilize preestablished atherosclerotic lesions by reducing MMP expression within the lesion. (*Arterioscler Thromb Vasc Biol.* 2000;20:70-79.)

Key Words: atherosclerosis ■ ACAT ■ matrix metalloproteinases ■ macrophages ■ plaque rupture

An integral process in the pathogenesis of atherosclerosis is the cholesteryl ester (CE) enrichment of the arterial wall. CE enrichment can occur by passive influx and extracellular deposition of plasma lipoproteins, active cellular metabolism, and active intracellular storage. In humans, arterial CE content increases from ≈2% to 50% of the total vessel lipid over 70 years,¹ with a change in the cholesteryl oleate-linoleate ratio from 0.8 to 2.9.² The change in fatty acyl pattern is a reflection of a change in the relative amounts of lipoprotein-derived CE, cholesteryl linoleate, and acyl-CoA:cholesterol *O*-acyltransferase (ACAT)-derived cholesteryl oleate.² Brown and Goldstein³ have shown that in the 2-compartment model of CE cycling in the macrophage, lipoprotein-derived cholesteryl linoleate is hydrolyzed and the free cholesterol is reesterified with oleoyl-CoA by ACAT to form intracellular cholesteryl oleate-enriched lipid droplets. Concomitant with the changes in CE content and fatty

acyl pattern is the influx of monocytes-macrophages and smooth muscle cells.⁴ Thus, under conditions of excessive cholesterol accumulation in the vascular wall, ACAT, a primary enzyme responsible for cholesterol esterification, appears responsible for the generation of the hallmark of atherosclerosis, namely, the monocyte-macrophage foam cell.

Monocyte-macrophage foam cells have recently been implicated as playing a role in atherosclerotic lesion destabilization and rupture. With atherosclerotic lesion development, there is an increase in the expression of matrix metalloproteinase (MMP) -1, MMP-3, MMP-7, and MMP-9.⁵⁻⁹ Specifically, both MMP-1 and MMP-7 have been identified in macrophage-rich regions of human carotid lesions.^{5,7} MMP-9 has been seen in atherectomy specimens from individuals with unstable angina⁹ and associated with macrophage-rich regions of lesions obtained at surgery or autopsy.^{5,6} In addition, MMPs have been shown to be catalytically active

Received October 21, 1998; revision accepted May 22, 1999.

From the Departments of Cardiovascular Therapeutics (T.M.A.B., B.R.K., W.S.R., S.B.M., X.L., C.D., T.M.), Pharmacokinetics and Drug Metabolism (C.L.), and Chemistry (H.L.), Parke-Davis Pharmaceutical Research, Division of Warner-Lambert, 2800 Plymouth Rd, Ann Arbor, Mich.

Correspondence and reprint requests to Thomas M.A. Bocan, PhD, Department of Cardiovascular Therapeutics, Parke-Davis Pharmaceutical Research, Division of Warner-Lambert, 2800 Plymouth Rd, Ann Arbor, MI 48105. E-mail thomas.bocant@wl.com

© 2000 American Heart Association, Inc.

Arterioscler Thromb Vasc Biol. is available at <http://www.atvbaha.org>

when evaluated by gelatin or casein zymography, and both the gelatinolytic and caseinolytic activities have been localized to the shoulders of atherosclerotic lesions in areas of monocyte-macrophage accumulation.⁶ Because macrophages are a source of MMPs, one might conclude that pharmacological agents capable of reducing the amount of macrophages within atherosclerotic lesions could act to stabilize the developing lesion if MMPs are the primary enzymes involved in vascular matrix remodeling.

Given the involvement of ACAT in atherosclerotic lesion development and macrophage foam cell formation, inhibitors of ACAT have been evaluated for their antiatherosclerotic activity. Such agents have been shown to effectively reduce lesion development but to varying degrees; however, in almost every study, interpretation of the data was confounded by changes in plasma total cholesterol.^{10–13} When plasma total cholesterol levels were unaltered by drug administration and systemic levels of drug were achieved, rather striking reductions in lesion extent, CE enrichment, and macrophage foam cell involvement were noted.¹⁴ In the studies cited above, the various ACAT inhibitors were administered in a cholesterol-containing diet, and the compounds were shown to limit the development of the macrophage-enriched fatty streak or fibrofoamy lesions. In contrast to previous studies, we sought to evaluate the effect of the ACAT inhibitor avasimibe, in a model in which advanced, fibrous, plaque-like lesions develop. To develop advanced atherosclerotic lesions and limit the effect of plasma cholesterol lowering on changes in lesion end points, rabbits were switched from a cholesterol/fat diet to a chow/fat diet before administration of avasimibe. Previous studies had indicated that in rabbits, reductions in plasma cholesterol levels tend to result in an advancement of atherosclerotic lesions rather than regression of atherosclerosis.^{15,16} Because monocytes-macrophages and matrix-degrading enzymes are localized to the potentially friable shoulder regions of atherosclerotic lesions, we characterized the effect of avasimibe not only on the extent and composition of the developing lesion but also on the expression of MMPs and of tissue inhibitor of matrix metalloproteinase (TIMP)-1 and -2 within the lesion.

Methods

Experimental Design

Male New Zealand White rabbits from Kuiper Farms (Gary, Ind) weighing 1.2 to 1.5 kg were fed chow diet meals (Purina 5321) supplemented with 0.5% cholesterol, 3% peanut oil, and 3% coconut oil diet for a total of 9 weeks, followed by a 0% cholesterol, 3% peanut oil, and 3% coconut oil diet (chow/fat diet) for 6 weeks before a 7- to 8-week administration of the ACAT inhibitor avasimibe, which was formerly known as CI-1011, in the chow/fat diet. The dietary regimen consisted of feeding 30 g for the first week, 40 g for 2 weeks, 50 g for 2 weeks, 60 g for 4 weeks, 70 g for the next 6 weeks, and 80 g for the final 7 to 8 weeks. After 1 week of diet initiation, chronic endothelial injury was induced in the abdominal aorta and femoral artery by surgically inserting a sterile, indwelling, 18-cm nylon monofilament with a diameter of 200 μm into the lumen of the right femoral artery. Surgical procedures were performed on animals anesthetized with 10 mg/kg xylazine from Miles and 33 mg/kg ketamine HCl from Fort Dodge Laboratories in accordance with a vertebrate use form approved by the Parke-Davis institutional review board. After the initial 15-week lesion-induction phase, which consisted of both hypercholesterolemia and a dietary normalization phase, animals were assigned on the basis of their 24-hour postmeal plasma total cholesterol values to the experimental

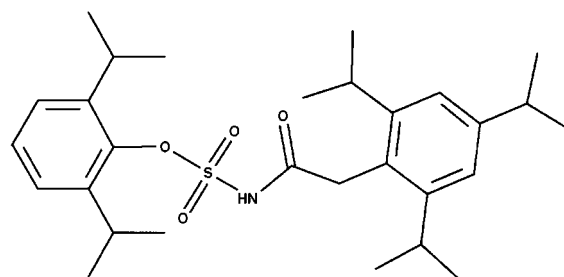


Figure 1. Chemical structure of the ACAT inhibitor avasimibe, which is a [[2,4,6-tris(1-methylethyl)phenyl]acetyl]sulfamic acid, 2,6-bis(1-methylethyl)phenyl ester.

groups such that there were no statistical differences in plasma cholesterol levels. A total of 48 animals were used. One group of animals, hereafter referred to as the time 0 controls ($n=16$), was necropsied before drug administration while a second group, termed the progression controls ($n=16$), was maintained on the chow/fat diet for the remaining 7 to 8 weeks of the study. An additional group ($n=16$) of animals was given 25 mg/kg avasimibe as an admixture to the chow/fat diet for the next 7 to 8 weeks. Plasma and vascular lipid levels and histological and morphometric measurements were made on all animals. Plasma and tissue drug levels ($n=8$) as well as vascular MMP expression were assessed in a subset of animals, ie, $n=4$ to 6 by MMP zymography and $n=8$ by Northern analysis for MMP and TIMPs. The structure (Figure 1), synthesis, and *in vitro* activity of avasimibe were previously reported.¹⁷ The drug diet was freshly prepared on a biweekly basis.

Biochemical Methods

Plasma total cholesterol and triglyceride levels were measured enzymatically throughout the study on an Abbott series II bichromatic analyzer^{18,19} with the Boehringer Mannheim total cholesterol reagent and the Abbott triglyceride reagent. The lipid measurements were made monthly or biweekly throughout the study on plasma samples collected 24 hours after a meal.

Plasma and vascular avasimibe concentrations were obtained in a group of 8 animals receiving 25 mg/kg avasimibe for 7 to 8 weeks that were not used for the morphological and biochemical measurements; however, gross lesion extents were comparable in both avasimibe treatment groups. Plasma samples from avasimibe-treated animals were obtained after 7 weeks of dosing at 0, 1, 2, 4, 8, and 24 hours postdose, and plasma concentrations were determined by use of a liquid chromatographic–mass spectrometric assay. Avasimibe and the internal standard [¹³C₆]CI-1011 were extracted from plasma with diethyl ether. The ether layer was evaporated to dryness and the residue reconstituted in acetonitrile/water (70:30, vol/vol). The chromatography conditions consisted of a 2.1×150-mm×5- μm Zorbax RX-C18 column with a mobile phase of acetonitrile/5 mmol/L ammonium acetate buffer (70:30, vol/vol) at a flow rate of 0.2 mL/min. Analytes were detected by mass spectrometry. Vascular avasimibe levels were quantified in a similar manner to that noted above for plasma; however, 100 to 200 mg of aortic arch tissue was homogenized in 2 to 4 mL of water before extraction with diethyl ether. Aortic arch samples were collected 24 hours postdose after 8 weeks of 25 mg/kg avasimibe.

A 3-cm segment of the iliac-femoral artery adjacent to that collected for histological evaluation and the descending thoracic aorta were assayed for their total cholesterol, CE, free cholesterol, and total phospholipid content as previously described.²⁰ The lipids were extracted in chloroform/methanol (2:1, vol/vol) by the procedure of Folch et al.²¹ The lipid composition of the iliac-femoral artery and descending thoracic aorta was measured with an Iatroscan TH-10 Mark IV thin-layer chromatography–flame ionization detection analyzer from RSS Inc attached to a Hewlett-Packard 3390A integrator.²⁰

Macrophage Cell Culture Methods

The IC₅₀ of avasimibe against macrophage ACAT was evaluated in cultured human monocyte-derived macrophages. Human mono-

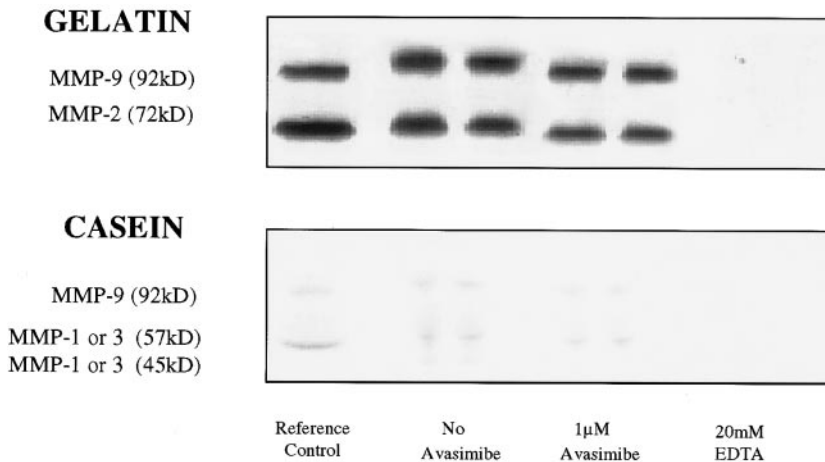


Figure 2. Inhibition of zymogen bands within gelatin and casein gels by 20 mmol/L EDTA and lack of MMP inhibition with 1 μ mol/L avasimibe. The digital image was inverted for better definition of the zymogen bands, so the bands appear dark rather than clear.

cyte-derived macrophages supplied by Advanced Biotechnology, Inc (Columbia, Md) were elutriated from the blood of healthy adult donors as previously described.²² Frozen but viable monocytes (20×10^6 cells per vial) were thawed and plated into 6-well plates containing RPMI 1640 medium, 10% FBS obtained from HyClone Laboratories, and 1 ng/mL granulocyte macrophage colony-stimulating factor (GM-CSF) from R&D Systems for 10 days to promote monocyte differentiation. On day 10, the cells were washed and incubated with RPMI 1640, 1% Hu-Nutridoma from Boehringer Mannheim, and 1 ng/mL GM-CSF for an additional 24 hours. The culture medium was changed from RPMI 1640 with 1% pen/strep, 10% FBS, and 1 ng/mL GM-CSF to RPMI 1640 with 1% pen/strep, 1% Hu-Nutridoma, and 1 ng/mL GM-CSF. Avasimibe was dissolved in dimethyl sulfoxide and was added at concentrations of 10 to 1000 nmol/L for 1 hour before the addition of 37 μ g/mL acetylated LDL supplied by PerImmune, Inc. After a 24-hour incubation the internal standard, 1,2-hexadecanediol (Aldrich Chemical Co), was added at 37.5 μ g/mL to each well, and lipids were extracted with 1 mL of hexane/isopropanol (3:2, vol/vol). After extraction, the organic phase was dried under N_2 and redissolved in isoctane/tetrahydrofuran (97:3, vol/vol), and the free cholesterol, CE, and triglyceride content of the cells was quantified with a high-performance liquid chromatography method.²³ In separate cultures treated in a similar fashion to that noted above for determination of the IC_{50} of avasimibe against macrophage ACAT, the medium was removed and MMP activity was assessed by gelatin zymography.

Zymography Methods

Aortic MMP expression was assessed in the aortic arch of 4 to 6 animals from the progression control and avasimibe treatment groups. Specimens of aortic arch were stored at -70°C before extraction of tissue MMPs according to the procedure described by Galis et al.⁶ Tissue samples were minced and homogenized in ice-cold 10 mmol/L sodium phosphate buffer (pH 7.2) containing 150 mmol/L NaCl, 1% Triton X-100, 0.1% SDS, 0.5% sodium deoxycholate, and 0.2% NaN_3 . Tissue homogenates were centrifuged at 14 000 rpm for 10 minutes at 4°C and the supernatant was collected. Protein content was measured by a Bio-Rad protein assay,²⁴ and SDS-polyacrylamide gel electrophoresis zymography was performed on the extracted tissue specimens.⁶ One part of tissue homogenate containing 30 μ g of protein was mixed with 1 part of $2 \times$ SDS sample buffer from Novex, and molecular weight markers were added. Each sample was loaded on either a 10% polyacrylamide gel containing 0.1% gelatin purchased precast from Novex or a 4% to 16% acrylamide gel containing β -casein, which was prestained for protein from Novex. As a positive control, lysates of cultured rabbit renal artery smooth muscle cells treated with 4 mmol/L phorbol 12-myristate 13-acetate for 18 hours and known to express MMP-2, -3, and -9 were added to each gel. After electrophoresis at 125 V for 90 minutes, the gel was renatured in renaturing buffer from Novex for 30 minutes. After equilibration in the Novex developing buffer for 30 minutes, fresh developing buffer was added, and the gelatin-containing gel was allowed to develop

overnight at 37°C while the casein-containing gels were developed for 72 hours at 37°C to visualize the zymogen bands. The gelatin gels were stained with 0.5% Coomassie blue and destained with buffer consisting of 10% acetic acid, 50% methanol, and 40% distilled water for 30 minutes to visualize the zymogen bands. An image of each gel was scanned into a computer with a Hewlett-Packard scanner, and the zymogen bands were quantified by using Biosoft QuantiScan software; results are expressed in arbitrary densitometric units. Because MMP-1 and MMP-3 could not be differentiated on the casein-impregnated gel owing to their similar electrophoretic mobilities, the zymogen bands at 57 and 45 kDa were considered to represent latent and active forms of both MMPs. An antibody specific for rabbit MMP-3 obtained from Calbiochem indicated by Western analysis that the zymogen bands at 57 and 45 kDa contained MMP-3; however, the presence of MMP-1 could not be ruled out, since a specific antibody to rabbit MMP-1 was not available. A faint band at 19 kDa or MMP-7 was also observed in the casein gels; however, the band intensity precluded reproducible densitometric quantification. To validate that the zymogen bands were MMPs, 0.2 to 20 mmol/L EDTA was added to the developing buffer of several control lanes. Catalytic activity was abolished on incubation with EDTA; however, addition of 1 μ mol/L avasimibe to the developing buffer had no effect on the formation of the zymogen bands (Figure 2).

Molecular Methods

Total RNA was extracted with a guanidine isothiocyanate method²⁵ in both progression control and avasimibe-treated animals ($n=8$ per group). RNA (20 μ g) was electrophoresed in a 1% formaldehyde/agarose gel and blotted onto a nylon membrane (Schleicher & Schuell) in $20 \times$ SSC by capillary transfer overnight. The Northern blot was baked at 80°C for 20 minutes, UV cross-linked, and prehybridized. Blots were hybridized at 65°C with radiolabeled [α - ^{32}P]dCTP cDNA probes for rabbit MMP-2, MMP-9, TIMP-1, TIMP-2 and, as an internal control, human S9 ribosomal cDNA (0.9 kb). The probes were generated by reverse transcriptase-polymerase chain reaction from rabbit tissue RNA by using sense and antisense primers (Life Tech) as listed in Table 1. The membranes were washed at 65°C in 1% SDS/ $2 \times$ SSC, and the signals were quantified by using a Storm 860 PhosphorImager and ImageQuant software (Molecular Dynamics).

Cytochemical Methods

For histological evaluation of the iliac-femoral and aortic arch lesions, the first 1-cm segment of the iliac-femoral artery distal to the aortic-iliac bifurcation and the ascending aorta distal to the aortic valves, respectively, were fixed in 10% neutral buffered formalin for 24 hours. The vessels were dehydrated, cleared in xylene, and infiltrated with molten paraffin ($<60^\circ\text{C}$) by using a Miles Scientific Tissue-Tek VIP autoproccessor. The tissue segments were embedded in paraffin and sectioned at 5 μ m with a Reichert-Jung microtome purchased from Baxter. To obtain a thorough representation of the histological appearance of the iliac-femoral lesion, 3 ribbons of 20 sections each were cut. Each ribbon of sections was spaced

TABLE 1. Sense and Antisense Primers Used to Isolate Rabbit MMP-2, MMP-9, TIMP-1, and TIMP-2

Target	Sense Primer	Antisense Primer	Fragment, bp
MMP-2	TTGGATCCTCTACAGCAG	AAGAATCCCGTAGAGCT	500
	CTGCACCAG	CTTGAATGC	
MMP-9	AAGGATCCAGTTTCGGTTC	AAGAATTCGGCGCCGGTA	600
	ATCTTCCAG	GGGCTGGTA	
TIMP-1	GGATTCACCATGGCCCC	GAGCAGCCTTCAGTCTTTC	650
	TTGGC	CGGGCCGCAGGGACT	
TIMP-2	AAATTAATCATATGTGCA	GCTTACGGGTCCTCGATGT	600
	GCTGCTCCCGGTGCAC	C	

≈100 μm apart. Three pairs of sections, ie, 1 pair from each ribbon, were affixed to cleaned, 3-aminopropyltriethoxysilane-coated glass slides and stored until stained. The general histological character and nature of the extracellular matrix were evaluated in hematoxylin- and eosin- and Verhoeff's elastica-stained sections.²⁶ The cellular composition of lesions was determined by using anti-RAM11 antibodies to rabbit monocytes-macrophages from Dako²⁷ and an anti-HHF35 smooth muscle cell antibody from Enzo Diagnostics.²⁸ The immunocytochemical staining of monocytes-macrophages and smooth muscle cells was performed as described previously.²⁹

Morphometric Methods

Sections of the iliac-femoral artery, a site of the diet plus chronic injury-induced atherosclerosis, and the aortic arch, a reproducible and predictable site of hypercholesterolemia-induced lesions, were stained by using Verhoeff's elastica procedure or with immunocytochemical markers for monocytes-macrophages and used for quantification of lesion and monocyte-macrophage areas as well as monocyte-macrophage size. Given the lack of a predictable site for atherosclerotic lesion formation in the descending thoracic aorta, no histological measurements were made of lesions in this region. Gross extent of atherosclerosis within the thoracic aorta was also measured. The morphometric analyses of the iliac-femoral artery were performed on a Power Macintosh 8100/80AV computer using the public domain National Institutes of Health (NIH) Image program (written by Wayne Rasband at the US NIH and available from the Internet by anonymous ftp from zippy.nimh.nih.gov or on floppy disk from NTIS, 5285 Port Royal Rd, Springfield, VA 22161, part PB93-504868). Morphometric analyses of the aortic arch and thoracic aorta were performed by using a PGT Imagist II image analysis system as previously described.²⁹ Quantification of monocyte-macrophage size was performed on RAM11-stained, hematoxylin-counterstained sections by using Image Pro Plus image analysis software (Media Cybernetics). Images of 10 random and nonoverlapping fields of RAM11-positive areas within aortic arch cross sections were collected at ×40 on a Leica DMR microscope from each control and avasimibe-treated animal. Areas of RAM11-positive staining and the number of nuclei associated with the immunoprecipitate were quantified, and average monocyte-macrophage cell area was calculated.

Iliac-femoral and aortic arch lesion and macrophage areas and aortic arch macrophage size were determined for each specimen, and the average per group was calculated based on the mean specimen area. The percent lesion coverage of the thoracic aorta was also determined for each group.

Statistical Analyses

All statistical comparisons of the biochemical and morphometric data were made relative to the untreated, hypercholesterolemic progression controls. Total plasma cholesterol exposure of the animals over the course of the study and during the drug treatment phase were determined by applying the trapezoidal rule³⁰ to the cholesterol-time curves. An ANOVA procedure followed by a least significant difference test or a 1-tailed Student's *t* test for comparisons made relative to the untreated progression controls was used.

To ensure an unbiased result, the data were collected in a double-blinded fashion. The specimens were ascribed to their respective treatment group after the biochemical and morphometric measurements were obtained.

Results

During the hypercholesterolemia phase, ie, the first 9 weeks of the study, plasma total cholesterol levels rose to between 1500 and 2000 mg/dL but decreased to ≈500 mg/dL during the subsequent 6-week dietary normalization phase (Figure 3A). At necropsy, mean plasma total cholesterol levels were reduced 70% by avasimibe; however, no significant changes were noted at previous time points. Before drug treatment, plasma total cholesterol exposure as measured by the area under the cholesterol-time curve was similar between control and avasimibe groups, ie, 117 792 and 104 422 mg · d/dL, respectively. Avasimibe had no effect on plasma total cholesterol exposure during the final 8-week treatment phase (Figure 3B). Plasma triglyceride levels were unaffected by avasimibe treatment, and mean triglyceride values ranged from 46 to 169 mg/dL.

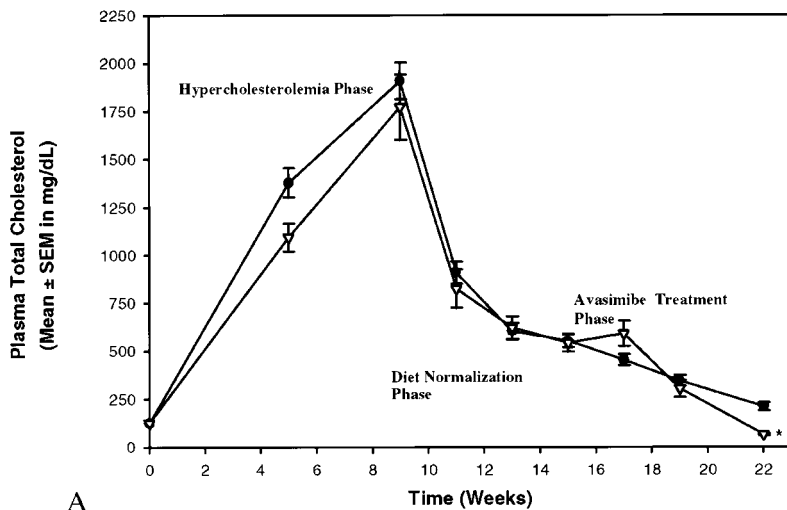
Plasma avasimibe maximal concentrations determined in a subset of animals treated with 25 mg/kg avasimibe for 7 weeks but comparably fed the fat diet was 178±31 ng/mL (mean±relative standard deviation %) while the plasma 24-hour area under the curve was 2525±33 ng · h/mL. In extracts of aortic arch taken 24 hours postdose after 8 weeks of 25 mg/kg avasimibe treatment, these concentrations were 25 ng/g of tissue wet weight.

In cultured human monocytes-macrophages, avasimibe reduced the intracellular CE concentration in a dose-dependent manner while free cholesterol and triglyceride concentrations were relatively unchanged over the range of 10 to 1000 nmol/L avasimibe. The IC₅₀ of avasimibe against isolated, cultured, primary human monocyte-macrophage ACAT was 25±9 nmol/L, or 12±4.5 ng/mL (mean±SEM).

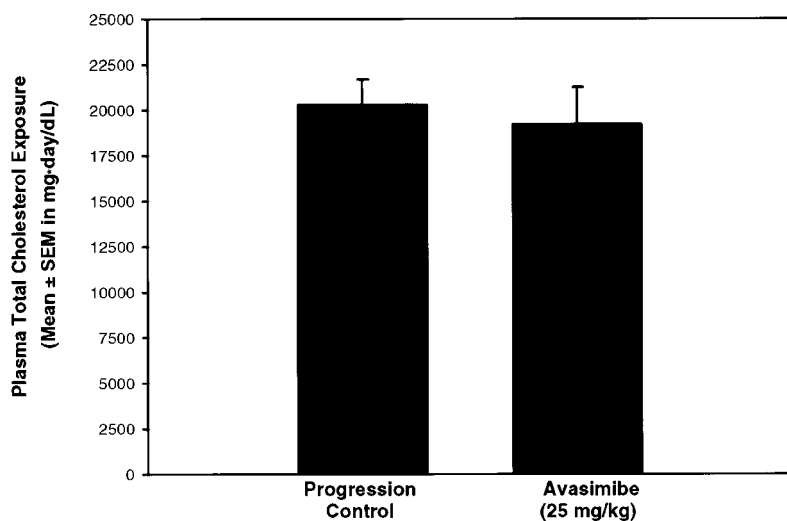
Thoracic aortic and iliac-femoral CE contents were reduced by 39% and 36%, respectively, by avasimibe relative to the untreated control and by 25% and 39%, respectively, when compared with time 0, ie, initiation of drug intervention (Table 2). Thoracic aortic free cholesterol content was reduced by 39%; however, no change in total phospholipid content or free cholesterol was noted in the iliac-femoral artery.

Aortic arch MMP levels as measured by gelatin and casein zymography were reduced after avasimibe treatment (Figure 4). The density of the zymogen bands associated with 92-kDa (latent MMP-9) and 88-kDa (active MMP-9) gelatinases was reduced by 65% and 33%, respectively. The density of bands associated with 72-kDa (latent MMP-2) and 66k-Da (active MMP-2) gelatinases was modestly reduced by 7% to 20%, but such changes were not statistically significant. Density of the zymogen bands on the casein gels associated with 57-kDa material (latent MMP-1 and -3) was reduced 52% and with 45-kDa material (active MMP-1 and -3) was decreased 60%. Cultured, human monocyte-macrophage MMP levels as measured by gelatin zymography were unaffected by direct administration of avasimibe to the cultures.

After a 24-hour incubation with 50 μg/mL acetyl-LDL, macrophage CE and free cholesterol content as determined by high performance liquid chromatography was 45% and 55%,



A



B

Figure 3. A, Mean plasma total cholesterol levels over the course of the study. The final plasma cholesterol value is significantly different from control at $P < 0.05$. ●, Progression control; ▽, 25 mg/kg avasimibe. B, Mean plasma total cholesterol exposure during the final 7-week treatment phase. No significant differences were noted at $P < 0.05$.

respectively, of total cholesterol. Latent MMP-9 and MMP-2 were present in differentiated non-CE-enriched human monocyte-derived macrophages, and no change in the amount of catalytic activity was noted after incubation with acetyl-LDL for 24 hours. The catalytic activity was inhibited by incubation with EDTA. Direct incubation of up to 1000 nmol/L avasimibe with cultured human monocytes-macrophages had no effect on latent MMP-9 and MMP-2 catalytic activity.

Changes in aortic arch MMP and TIMP expression as measured by Northern analysis were also noted on avasimibe

treatment (Figure 5 and Table 3). Aortic arch MMP-2 mRNA levels increased 135% while MMP-9, TIMP-1, and TIMP-2 mRNA levels decreased an average of 28% to 39% after avasimibe treatment.

Histological evaluation of the aortic arch and iliac-femoral artery revealed that the atherosclerotic lesions were of several distinct morphological appearances. In both vascular regions, the lesions were macrophage and smooth muscle cell enriched; however, the relative distribution and quantity of these cell types varied. In the aortic arch, the macrophages were located both superficially and within the deep intimal

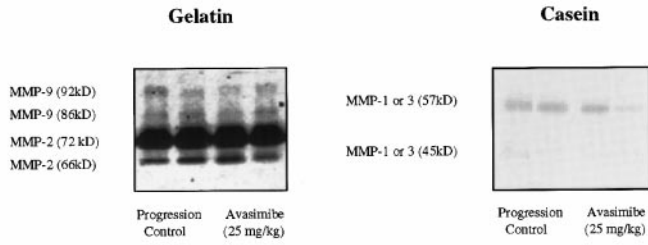
TABLE 2. Thoracic Aortic and Iliac-Femoral Lipid Content

Treatment	Thoracic Aorta			Iliac-Femoral Artery		
	CE	Free Cholesterol	Total Phospholipids	CE	Free Cholesterol	Total Phospholipids
Time 0 control	148.1±20.7	57.9±6.3	49.9±3.0	181.0±20.8	56.9±3.8	39.3±3.1
Progression control	179.7±17.7	84.9±8.8	63.6±5.0	170.6±13.4	56.7±6.3	38.6±2.7
Avasimibe, 25 mg/kg	110.6±19.4*	51.7±11.4*	56.2±6.6	110.1±16.4*	51.3±6.4	35.9±7.0
	(-39)	(-39)	(-12)	(-36)	(-10)	(-7)

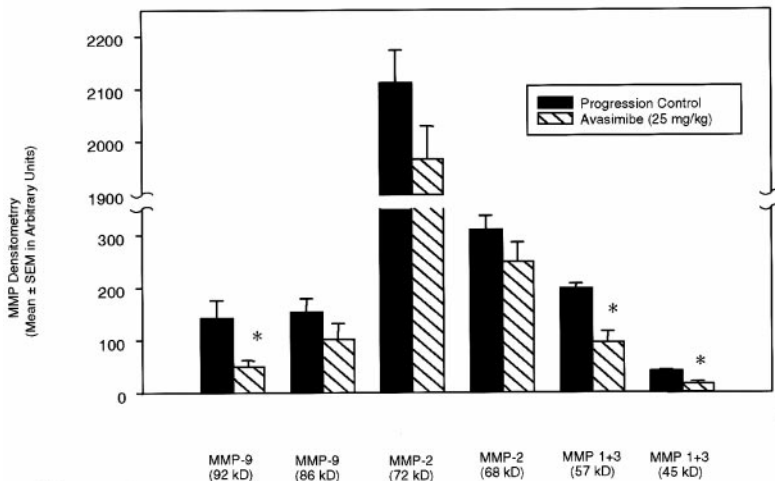
Data are expressed as mean±SEM in $\mu\text{g}/\text{mg}$ dry defatted tissue. $n=16$ in the time 0 and progression groups and 8 in the avasimibe treatment group. Values in parentheses represent percent change from progression control.

*Statistically significant difference from the progression control group.

Downloaded from <http://atvb.ahajournals.org/> by on April 15, 2008



A.



B.

Figure 4. MMP expression in the aortic arch of hypercholesterolemic rabbits treated with 25 mg/kg avasimibe. A, Gelatin zymography (left) depicts the catalytic activity at 92, 86, 72, and 66 kDa in control and avasimibe-treated animals. Casein zymography (right) depicts the effect of avasimibe on the catalytic activity at 57 and 45 kDa. The digital image was inverted for better definition of the zymogen bands, so the bands appear dark rather than clear. B, Bar graph representing the density of the various zymogen bands expressed as the mean ± SEM in arbitrary densitometry units. Statistically significant differences from the progression control at $P < 0.05$ are noted.

regions of the lesion, whereas in the iliac-femoral artery, the macrophages were predominantly located in the deep intimal and medial regions. The degree of lesion complexity, as evidenced by the incidence of fibrous plaques and fibrofoamy lesions, varied with the vascular region and treatment group. Fibrous plaque lesions were identified as areas containing basophilia and intimal necrosis, cholesterol clefts, and/or calcium deposits. Fibrofoamy lesions were characterized as macrophage- and smooth muscle cell-enriched lesions without evidence of intimal necrosis. In the aortic arch, 50% to 62% of the progression control and drug-treated animals had fibrous plaque lesions, whereas 94% of the animals in the time 0 group had macrophage-enriched fibrofoamy lesions. In the iliac-femoral artery, avasimibe decreased the incidence of fibrous plaque lesions from 50% to 28% of the animals.

Morphometric measures of atherosclerotic lesion extent and composition were also altered. Relative to drug initiation, thoracic aortic, aortic arch, and iliac-femoral lesion size or extent and monocyte-macrophage enrichment increased in control animals administered the chow/fat diet alone. Avasimibe reduced the percent lesion coverage of the thoracic aorta from 34% in the control animals to 20%. Avasimibe decreased the cross-sectional lesion area and monocyte-macrophage content of the aortic arch by 35% and 27%, respectively (Figure 6). Monocyte-macrophage size within the aortic arch was unaffected by avasimibe treatment (Table 4). In the iliac-femoral artery, avasimibe decreased the monocyte-macrophage content of the lesion by 77% and the

ratio of RAM11-positive cell area to lesion area from 0.22 to 0.05 (Figure 7).

Discussion

Direct inhibition of arterial wall ACAT can potentially stabilize atherosclerotic lesions and prevent plaque rupture by limiting macrophage accumulation and reducing the expression of MMPs. This conclusion is supported by several findings of the current study, which can be summarized as follows: (1) Avasimibe decreased the cross-sectional lesion area and the monocyte-macrophage content of the foam cell-enriched aortic arch by 35% and 27%, respectively. The reduction in monocyte-macrophage area reflected a change in cell number and not cell size. (2) In the iliac-femoral artery, avasimibe specifically decreased the monocyte-macrophage content of the lesions by 77% and the ratio of RAM11-positive cell area to lesion area from 0.22 to 0.05. (3) In the absence of a reduction in plasma cholesterol exposure, avasimibe decreased thoracic aortic and iliac-femoral CE content by 39% and 36%, respectively. Because CE is the end product of the ACAT reaction, these data suggest that vascular ACAT was inhibited. (4) Plasma and tissue concentrations of avasimibe were 178 ng/mL and 25 ng/g of tissue weight wet, respectively. Such levels exceed those required to inhibit macrophage ACAT, ie, an IC_{50} of 24 nmol/L or 12 ng/mL, and further support the hypothesis that direct inhibition of vascular ACAT had occurred. (5) Aortic arch MMP activity as measured zymographically was reduced by 33% to

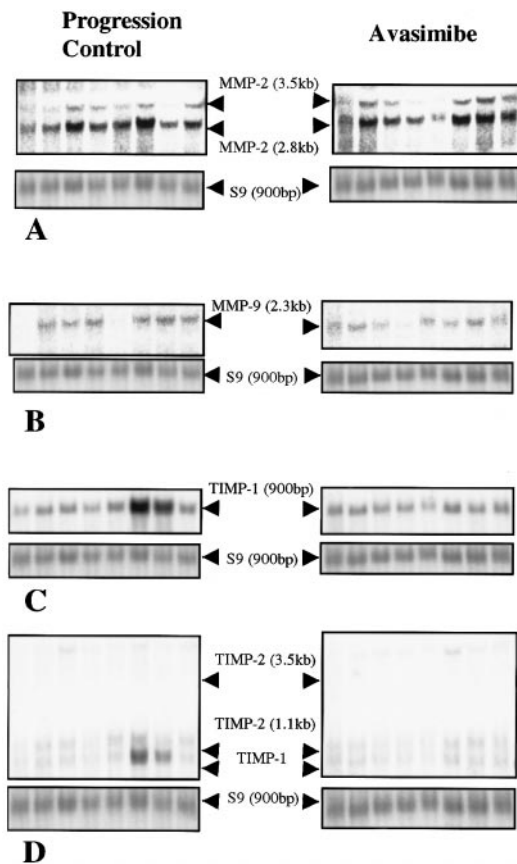


Figure 5. MMP and TIMP mRNA expression in the aortic arch of progression control and avasimibe-treated animals. S9 was used as a measure of equal loading. A, MMP-2; B, MMP-9; C, TIMP-1; and D, TIMP-2.

65%, and aortic arch MMP-9, TIMP-1, and TIMP-2 mRNA levels were decreased from 28% to 39%. Both groups of changes were associated with reductions in aortic arch macrophage area.

In contrast to hypolipidemic agents, ACAT inhibitors may directly modulate the development of atherosclerotic lesions. In the current study, plasma total cholesterol levels were primarily reduced by dietary intervention, and the degree of plasma cholesterol exposure was unaffected by avasimibe. It has been reported in rabbits that reductions in plasma cholesterol tend to result in an advancement of atherosclerotic lesions rather than a regression of atherosclerosis.^{15,16} The lack of lesion regression has been attributed to high rates of hepatic production of CE-rich VLDL after cessation of cholesterol feeding³² and the avid uptake of cholesterol by the aorta at even low plasma cholesterol levels.³³ The lack of

lesion regression after plasma cholesterol lowering is consistent with the observations of the current study. During the last 8 weeks of feeding a chow/fat diet, plasma total cholesterol levels in the untreated controls were reduced from ≈ 500 to 200 mg/dL while thoracic aortic lesion extent increased by 26% and aortic arch and iliac-femoral cross-sectional lesion areas increased by $\approx 50\%$. Avasimibe treatment resulted in similar changes in plasma total cholesterol; however, progression of the atherosclerotic lesions was prevented.

Avasimibe attenuated the development of atherosclerotic lesions by specifically altering the cellular composition of the lesions. In the aortic arch, lesions composed primarily of monocytes-macrophages as evidenced by a RAM11-positive cell to lesion ratio of 0.6 to 0.8 were reduced 27% to 35% by avasimibe. In addition, in the iliac-femoral artery where lesions were induced by chronic mechanical endothelial denudation, the area of monocytes-macrophages was markedly reduced by 77% without any change in the overall lesion cross-sectional area. Further evidence supporting a direct effect of avasimibe on arterial ACAT was the observation that the CE content of both the thoracic aorta, an extension of the aortic arch, and the iliac-femoral artery was reduced by 36% to 39%. Aortic arch levels of 25 ng of avasimibe per gram of tissue were also achieved in the animals at trough plasma levels. Such vascular drug levels can potentially inhibit macrophage ACAT in that the IC_{50} for inhibition of human monocyte-macrophage ACAT noted in the current study was 12 ng/mL and for mouse IC-21 cells, as published previously,¹⁷ was 30 ng/mL. Thus, one can conclude that a manifestation of inhibiting arterial wall ACAT is a selective reduction in monocyte-macrophage foam cells.

Reductions in arterial monocyte-macrophage foam cells may result in a structurally more stable atherosclerotic lesion. Although there was less atherosclerosis in the thoracic aorta and aortic arch of the avasimibe treated animals, the types of lesion that remained were fibromuscular or smooth muscle cell enriched. Monocyte-macrophage foam cell area in the iliac-femoral artery was not only reduced relative to the untreated progression controls but also was reduced 75% relative to a group of animals necropsied before drug administration. This latter finding suggests that ACAT inhibition may directly promote regression of atherosclerotic lesions rather than contribute to the deposition of free cholesterol within the necrotic core of the more advanced fibrous plaques. The reduction in monocytes-macrophages after avasimibe treatment could be a result of cells reentering the circulation, cell death, or apoptosis. Because there was no histological evidence of intimal necrosis or increased vascular lipid content after avasimibe treatment, it is unlikely that cell death accounted for the reduction in macrophages. Apoptosis is a potential mechanism for the reduction in monocytes-macrophages. Treatment of mouse peritoneal macrophages with the ACAT inhibitor SAH 58035 after loading by acetylated LDL has been shown to increase intracellular free cholesterol levels and promote apoptosis.³⁴ The lack of a change in vascular free cholesterol levels noted in the current study may be a consequence of limited sensitivity of the biochemical methods or that subtle changes in intracellular cholesterol pools caused by ACAT inhibition induce pathways responsible for promoting reverse cholesterol transport. In addition, unlike previous studies¹⁰⁻¹³ in

TABLE 3. MMP and TIMP mRNA Levels in the Aortic Arch of Control and Avasimibe-Treated Animals

	Progression Control	Avasimibe, 25 mg/kg
MMP-2	1.11 \pm 0.27	2.61 \pm 0.26*
MMP-9	1.33 \pm 0.35	0.96 \pm 0.14
TIMP-1	1.57 \pm 0.42	1.11 \pm 0.21
TIMP-2	1.22 \pm 0.08	0.88 \pm 0.03*

The data have been normalized for loading of the gel based on S9 content and are expressed as mean \pm SEM, n=8 per group.

*Statistically significant difference from the progression control at $P < 0.05$.

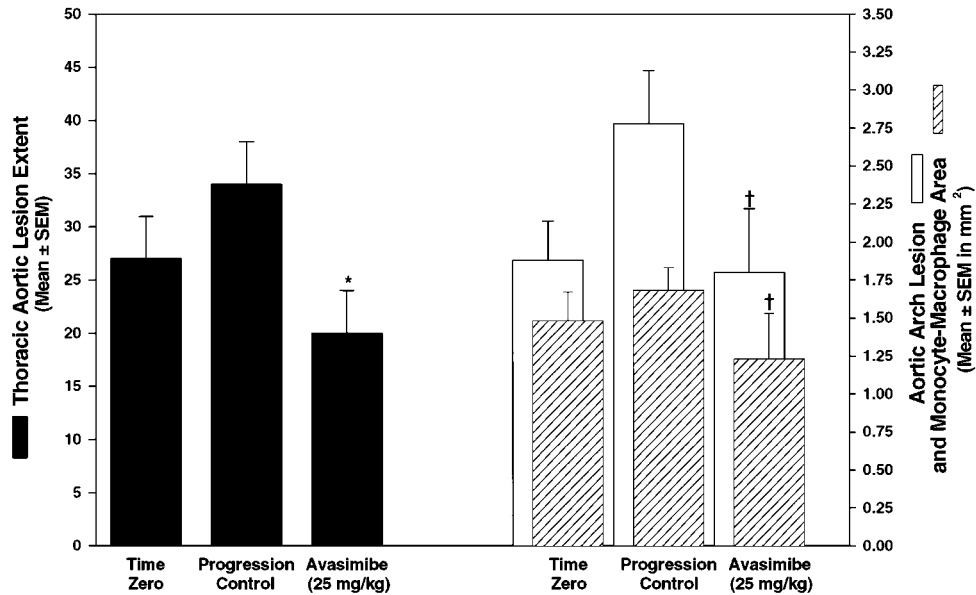


Figure 6. Morphometric evaluation of the extent of atherosclerosis within the thoracic aorta and the cross-sectional lesion and macrophage areas within the aortic arch. Statistically significant differences from the progression control at * $P < 0.05$ and † $P < 0.10$ are denoted.

which ACAT inhibitors were evaluated and wherein the predominant atherosclerotic lesion type even at the end of the study was that of a fatty streak or fibrofoamy lesion, in the current study, 50% to 60% of the animals had histological evidence of fibrous, plaquelike lesions within the aortic arch and iliac-femoral artery. Avasimibe reduced the incidence of fibrous plaques in the iliac-femoral artery from 50% to 28% of the animals. Therefore, one can suggest that selective reductions in lesion macrophage content could result in a coincident decrease in expression of proatherosclerotic molecules responsible for lesion progression and destabilization.

MMP expression, a potential proatherosclerotic event, has been associated with macrophage-rich shoulder regions of atherosclerotic lesions^{5,7} and circumstantially implicated in plaque rupture.⁵ MMP-1, -3, and -9 have been identified in macrophage-rich regions of human carotid lesions,⁵⁻⁷ atherectomy specimens from individuals with unstable angina,⁹ and associated with macrophage-rich regions of lesions obtained at surgery or autopsy.^{5,6} In addition, catalytically active forms of these MMPs have been localized to the shoulders of atherosclerotic lesions in areas of monocyte-macrophage accumulation.⁶ In the current study, avasimibe reduced latent and active MMP-9, as measured zymographically, by 65% and 33%, respectively. Latent and active MMP-1 and -3 collectively were also decreased by 52% to 60%. MMP-2 catalytic activity was unaffected. In addition to

changes in catalytic activity, we noted that mRNA levels for MMP-9, TIMP-1, and TIMP-2 were also reduced. The lack of change in MMP-2 catalytic activity and the increased mRNA expression may be related to the observation that fibromuscular or smooth muscle cell-rich lesions, ie, a putative source of MMP-2, remained after avasimibe treatment. Coincident with the decrease in catalytically active MMP-1, -3, and -9 was a 27% to 35% decrease in aortic arch lesion size and monocyte-macrophage content. Given the coincident reductions in monocyte-macrophage accumulation and MMP expression, one might propose that inhibition of macrophage ACAT may not only attenuate lesion development but also prevent plaque rupture by altering the macrophage to smooth muscle cell ratio within the lesion.

Although the data in the current study suggest that reductions in arterial MMP activity are an indirect consequence of macrophage accumulation, one cannot totally rule out the possibility that inhibition of ACAT and CE accumulation may regulate MMP expression. Such a hypothesis would presume that the reductions in macrophage area noted in the current study were due to a reduction in monocyte-macrophage size and not the number of cells. Based on a qualitative assessment of the histology of the aortic arch and iliac-femoral lesions, there were no visible differences in the appearances and relative sizes of the macrophages within the control or avasimibe-treated animals. Quantification of macrophage size in control and avasimibe-treated animals further indicated that there was no difference in cell size, which would suggest that the decrease in macrophage area was due to a reduction in cell number. One might propose that ACAT inhibition had a direct role in reducing MMP activity before the observed decrease in cell number; however, in vitro studies with primary human monocytes-macrophages tend to indicate the contrary. Addition of avasimibe to human monocytes-macrophages on loading with acetyl-LDL had no effect on the gelatinolytic activity of the collected media. In addition, avasimibe had no direct effect on MMP catalytic

TABLE 4. Aortic Arch Monocyte-Macrophage Size

Treatment	Average Macrophage Size, μm^2
Time 0 control	362 ± 41
Progression control	300 ± 26
Avasimibe, 25 mg/kg	281 ± 30

Data are expressed as mean ± SEM. n=16 in the time 0 and progression groups and 8 in the avasimibe treatment group. No statistically significant differences in average macrophage size were noted at $P < 0.05$.

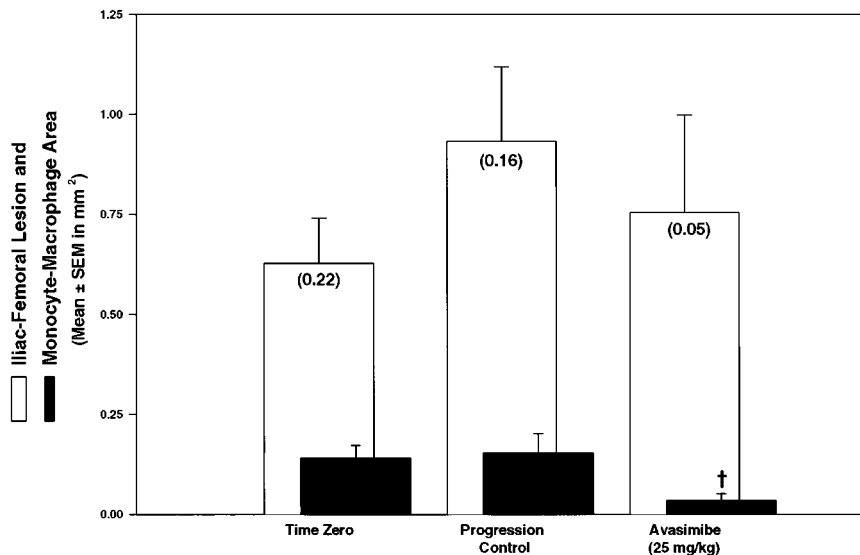


Figure 7. Morphometric evaluation of the iliac-femoral cross-sectional lesion and macrophage areas. The value in parenthesis represents the ratio of RAM11-positive monocytes-macrophages to lesion area. Statistically significant differences from the progression control at † $P < 0.10$ are denoted.

activity when incubated with the gelatin or casein gels during development. While it is apparent that further in vitro studies may be necessary to better understand whether CEs regulate MMP expression, the results from the current study would tend to indicate that the reductions in vascular MMP activity, MMP expression, and TIMP expression after avasimibe treatment are a consequence of the reduction in monocytes-macrophages.

Finally, a major implication of the current study is that inhibition of ACAT may not only directly alter the progression of the fibrofoamy lesion by limiting its macrophage enrichment and expression of macrophage-derived proatherosclerotic molecules but also, through lesion remodeling, reduce the potential for plaque rupture associated with the elaboration of macrophage-derived MMPs. In addition, reductions in monocyte-macrophage accumulation within atherosclerotic lesions or alterations in the phenotype of the monocytes-macrophages may further limit the expression of proatherosclerotic molecules, which may account for lesion progression.

Acknowledgments

The authors would like to express their appreciation to Brian Sanchez and Andrew Robertson for their technical help in performance of several aspects of the study.

References

- Small D. Progression and regression of atherosclerotic lesions: insights from lipid physical biochemistry. *Arteriosclerosis*. 1988;8:103–129.
- Smith EB, Evans PH, Downham MD. Lipid in the aortic intima: the correlation of morphological and chemical characteristics. *J Atheroscler Res*. 1967;7:171–186.
- Brown MS, Goldstein JL. Lipoprotein metabolism in the macrophage: implications for cholesterol deposition in atherosclerosis. *Annu Rev Biochem*. 1983;52:223–261.
- Haust MD. The natural history of human atherosclerotic lesions. In: Moore S, ed. *Vascular Injury and Atherosclerosis*. New York, NY: Marcel Dekker; 1981:1–23.
- Galis ZS, Sukhova GK, Kranzhoefer R, Clark S, Libby P. Macrophage foam cells from experimental atheroma constitutively produce matrix-degrading proteinases. *Proc Natl Acad Sci U S A*. 1995;92:402–406.
- Galis ZS, Sukhova GK, Lark MW, Libby P. Increased expression of matrix metalloproteinases and matrix degrading activity in vulnerable regions of human atherosclerotic plaques. *J Clin Invest*. 1994;94:2493–2503.
- Nikkari ST, O'Brien KD, Ferguson M, Hatsukami T, Welgus HG, Alpers CE, Clowes AW. Interstitial collagenase (MMP-1) expression in human carotid atherosclerosis. *Circulation*. 1995;92:1398–1408.
- Halpert I, Sires UI, Roby JD, Potter-Perigo S, Wight TN, Shapiro SD, Welgus HG, Wickline SA, Parks WC. Matrilysin is expressed by lipid-laden macrophages at sites of potential rupture in atherosclerotic lesions and localizes to areas of versican deposition, a proteoglycan substrate for the enzyme. *Proc Natl Acad Sci U S A*. 1996;93:9748–9753.
- Brown DL, Hibbs MS, Kearney M, Loushin C, Isner JM. Identification of 92-kD gelatinase in human coronary atherosclerotic lesions: association of active enzyme synthesis with unstable angina. *Circulation*. 1995;91:2125–2131.
- Krause BR, Bocan TMA. ACAT inhibitors: physiologic mechanisms for hypolipidemic and anti-atherosclerotic activities in experimental animals. In: Ruffolo RR, Hollinger MA, eds. *Inflammation: Mediators and Pathways*. Boca Raton, Fla: CRC Press; 1995:173–198.
- Krause BR, Sliskovic DR, Bocan TMA. Emerging therapies in atherosclerosis. *Exp Opin Invest Drugs*. 1995;4:353–387.
- Roth BD. ACAT inhibitors: evolution from cholesterol-absorption inhibitors to antiatherosclerotic agents. *Drug Discovery Today*. 1998;3:19–25.
- Bocan TMA. Animal models of atherosclerosis and interpretation of drug intervention studies. *Curr Pharm Des*. 1998;4:39–53.
- Bocan TMA, Bak Mueller S, Uhlendorf PD, Newton RS, Krause BR. Comparison of CI-976, an ACAT inhibitor, and selected lipid-lowering agents for antiatherosclerotic activity in iliac-femoral and thoracic aortic lesions: a biochemical, morphological and morphometric evaluation. *Arterioscler Thromb*. 1991;11:1830–1843.
- Constantinides P, Booth J, Carlson G. Production of advanced cholesterol atherosclerosis in the rabbit. *Arch Pathol*. 1960;70:80–92.
- Constantinides P. Production of experimental atherosclerosis in animals. *J Atheroscler Res*. 1961;1:374–385.
- Lee HT, Sliskovic DR, Picard JA, Roth BD, Wierenga W, Hicks JL, Bousley RF, Hamelehle KL, Homan R, Speyer C, Stanfield RL, Krause BR. Inhibitors of acyl-CoA:cholesterol *O*-acyl transferase (ACAT) as hypocholesterolemic agents: CI-1011: an acyl sulfamate with unique cholesterol-lowering activity in animals fed noncholesterol-supplemented diets. *J Med Chem*. 1996;39:5031–5034.
- Allain CC, Poon LS, Chan CSG, Richmond W, Fu PC. Enzymatic determination of total serum cholesterol. *Clin Chem*. 1974;20:470–475.
- Bucolo G, David H. Quantitative determination of serum triglycerides by the use of enzymes. *Clin Chem*. 1973;19:476–482.
- Bocan TMA, Bak Mueller S, Uhlendorf PD, Ferguson E, Newton RS. Dietary and mechanically induced rabbit iliac-femoral atherosclerotic lesions. *Exp Mol Pathol*. 1991;54:210–217.
- Folch J, Lees M, Sloane-Stanley GH. A simple method for the isolation and purification of total lipids from animal tissue. *J Biol Chem*. 1957;226:497–509.
- Snell JC, Chernyshev O, Gilbert DL, Colton CA. Polyribonucleotides induce nitric oxide production by human monocyte-derived macrophages. *Arterioscler Thromb Vasc Biol*. 1997;17:369–373.

23. Homan R, Anderson MK. Rapid separation and quantitation of combined neutral and polar lipid classes by high-performance liquid chromatography and evaporative light-scattering mass detection. *J Chromatogr B*. 1998;708:21–26.
24. Bradford M. A rapid and sensitive method for the quantitation of microgram quantities of protein utilizing the principle of protein-dye binding. *Anal Biochem*. 1976;72:248–254.
25. Chomczynski P, Sacchi N. Single-step method of RNA isolation by acid guanidinium thiocyanate-phenol-chloroform extraction. *Anal Biochem*. 1987;162:156–159.
26. Thompson SW. *Selected Histochemical and Histopathological Methods*. Springfield, Mass: Charles C Thomas Publishing; 1966: 1–1639.
27. Tsukada T, Rosenfeld M, Ross R, Gown AM. Immunocytochemical analysis of cellular components in atherosclerotic lesions: use of monoclonal antibodies with the Watanabe and fat-fed rabbit. *Arteriosclerosis*. 1986;6:601–613.
28. Gown AM, Vogel AM, Gordon D, Lu PL. A smooth muscle-specific monoclonal antibody recognizes smooth muscle actin isozymes. *J Cell Biol*. 1985;100:807–813.
29. Bocan TMA, Mazur MJ, Bak Mueller S, Quenby-Brown E, Sliskovic DR, O'Brien P, Creswell MW, Lee H, Uhlendorf PD, Roth BD, Newton RS. Antiatherosclerotic activity of inhibitors of 3-hydroxy-3-methylglutaryl coenzyme A reductase in cholesterol-fed rabbits: a biochemical and morphological evaluation. *Atherosclerosis*. 1994; 111:127–142.
30. Shanks ME, Gambill R. *Calculus Analytic Geometry/Elementary Functions*. New York, NY: Holt Rinehart & Winston; 1973:1–748.
31. Ott L. *An Introduction to Statistical Methods and Data Analysis*. North Scituate, Mass: Duxbury Press; 1977:1–730.
32. Daugherty A, Schonfeld G, Sobel BE, Lange LG. Metabolism of very low density lipoproteins after cessation of cholesterol feeding in rabbits. *J Clin Invest*. 1986;77:1108–1115.
33. Ho KJ, Pang LC, Taylor CB. Mode of cholesterol accumulation in various tissues of rabbits with prolonged exposure to various serum cholesterol levels. *Atherosclerosis*. 1974;19:561–566.
34. Kellner-Weibel G, Jerome WG, Small DM, Warner GJ, Stoltenberg JK, Kearney MA, Corjay MH, Phillips MC, Rothblat GH. Effects of intracellular free cholesterol accumulation on macrophage viability: a model of foam cell death. *Arterioscler Thromb Vasc Biol*. 1998;18:423–431.